IEEE Access
Multidisciplinary ⋮ Rapid Review ⋮ Open Access Journal

Received January 11, 2022, accepted January 28, 2022, date of publication February 4, 2022, date of current version February 11, 2022.

Digital Object Identifier 10.1109/ACCESS.2022.3149055

Memory Storage Systems Utilizing Chaotic Attractor-Merging Bifurcation

SOU NOBUKAWA[1,2], (Member, IEEE), NOBUHIKO WAGATSUMA[3], HARUHIKO NISHIMURA[4], (Member, IEEE), KEIICHIRO INAGAKI[5], (Member, IEEE), AND TERUYA YAMANISHI[6]

[1]Department of Computer Science, Chiba Institute of Technology, Narashino, Chiba 275-0016, Japan
[2]Department of Preventive Intervention for Psychiatric Disorders, National Institute of Mental Health, National Center of Neurology and Psychiatry, Kodaira, Tokyo 187-8551, Japan
[3]Department of Information Science, Faculty of Science, Toho University, Funabashi, Chiba 274-8510, Japan
[4]Graduate School of Applied Informatics, University of Hyogo, Kobe, Hyogo 650-0047, Japan
[5]Department of Robotic Science and Technology, Chubu University, Kasugai, Aichi 487-8501, Japan
[6]AI & IoT Center, Department of Management Information Science, Fukui University of Technology, Fukui, Fukui 910-8505, Japan

Corresponding author: Sou Nobukawa (nobukawa@cs.it-chiba.ac.jp)

The work of Haruhiko Nishimura was supported by the JSPS KAKENHI for Scientific Research (C) under Grant 20K11976. The work of Teruya Yamanishi was supported by the JSPS KAKENHI for Scientific Research (C) under Grant 18K11450.

ABSTRACT In nonlinear dynamical systems with barriers/thresholds, the signal response against a weak external input signal is enhanced by an appropriate additive noise (stochastic resonance). In recent years, progress in the application of stochastic resonance shows that the existence of additive noise heightens the memory storage functions in memory elements using bistable oscillations even with extremely low power consumption. By not restricting the additive noise, the deterministic chaos (an internal fluctuation) induces a similar phenomenon known as chaotic resonance. Chaotic resonance appears in nonlinear dynamical systems and is accompanied by chaos–chaos intermittency, where the chaotic orbit intermittently transitions among separated attractor regions through attractor-merging bifurcation. Previously, a higher chaotic resonance sensitivity than that of stochastic resonance was reported in various types of systems. In this study, we hypothesize that chaotic-resonance-based memory devices can store information with lower power consumption than that of stochastic-resonance-based devices. To prove this hypothesis, we induced attractor-merging bifurcation in a cubic map system, which is the simplest model for the emergence of chaotic resonance. Thereafter, we adjusted the internal system parameter under a noise-free system as the chaotic resonance and applied stochastic noise similar to the condition for inducing stochastic resonance. The results of this study reveal that, even with weaker memory storage input signals, the former exhibits a higher memory storage capability than the latter. The approach using chaotic resonance could facilitate the development of memory devices that were hitherto restricted to the application of stochastic resonance.

INDEX TERMS Chaos–chaos intermittency, chaotic resonance, memory storage, stochastic resonance, synchronization.

I. INTRODUCTION

Considering recent developments in artificial intelligence (AI), neuromorphic computing, and big data analysis, the amount of data being stored is increasing exponentially [1]. To manage such large amounts of data, efforts are being made to develop data storage devices with high density and high-speed data transmission capability [2]. Such devices are typified by high-density/high-speed nonvolatile memory and utilize phase-change random access memory (PCRAM) and a combination of PCRAM and neuromorphic computing [3]–[6]. However, they must also have low power consumption to achieve a low-carbon society [7]–[9]. Therefore, memory storage devices with low power consumption are needed.

To develop such a device, the stochastic resonance mechanism [10] (reviewed in [11]–[13]), in which synchronization in nonlinear systems possessing a barrier/threshold under a weak external input signal is strengthened using an additive stochastic noise with suitable strength, must be

The associate editor coordinating the review of this manuscript and approving it for publication was Ye Zhou.

utilized [14], [15]. In particular, Ibáñez *et al.* and Stotland and Di Ventra showed that the existence of additive noise heightens memory functions in memory elements with bistable oscillations, even under scenarios with extremely low power consumption [14], [15]. Consequently, studies have actively investigated stochastic resonance for realizing stochastic memory devices with low power consumption [16]. In memory devices, memory elements possesses bistable states corresponding to "0" and "1." The elements are initialized to "0." Then, they are changed to "1" during the storage phase. In memory devices that use the stochastic mechanism resonance, the amplitude of the input signal required for the state transition can be reduced by the effect of noise.

Along with additive stochastic noise, the deterministic chaos of an internal system's fluctuations induces a phenomenon called chaotic resonance that is similar to stochastic resonance [17]–[25] (reviewed in [12], [13], [26]). In chaotic resonance, chaos–chaos intermittency (where the chaotic orbit hops intermittently among several attractors distributed in spatially different regions) synchronizes with a weak external input signal. The profile of synchronization degree follows a unimodal maximum peak around the attractor-merging bifurcation, which is the function that controls the internal system parameter for attractor-merging (reviewed in [12], [26]). The sensitivity against the weak input signal and synchronization degree in the chaotic resonance are superior to those of stochastic resonance [23], [27]. Although numerous studies have been conducted on chaotic resonance, investigations were limited to the evaluation of the response of steady periodic input signals [22], [23], [28]–[32]. Consequently, the transient response in chaotic resonance, such as the transition from "0" to "1" in memory devices, remains unclear.

In this study, we hypothesized that the state transition caused by chaotic resonance can realize a novel memory storage mechanism with lower power consumption than that of a mechanism based on the stochastic resonance effect. To prove this hypothesis, in our preliminary study [33], we confirmed that memory storage can be realized using the attractor-merging bifurcation in a cubic map system, which is the simplest model for the emergence of chaotic resonance [12], by adjusting the internal system parameter under a noise-free condition. However, the strength of the perturbation for transition in chaotic resonance, which relates to power consumption, has not been compared to that in the conventional approach that utilizes stochastic resonance [14], [15]. Additionally, the robustness of chaotic resonance to background noise and parameter setting error is not clearly understood. In this study, based on our preliminary study [33], we evaluated and compared the abilities of the chaotic and stochastic resonance approaches for memory storage.

II. MATERIALS AND METHODS

A. CUBIC MAP WITH INPUT SIGNALS

A discrete cubic map is a well-known and simple chaotic system with chaos–chaos intermittency, and it is used for evaluating chaotic resonance (reviewed in [12]). In this study, we used an assembly composed of N cubic maps with memory signals $c_i(t)$ ($i = 1, 2, \cdots, N$), a parameter setting error of Δa, and a Gaussian white noise of $D_a\xi(t)$. This is given by

$$x_i(t+1) = F(x_i(t)) - c_i(t) + D_a\xi(t), \tag{1}$$

$$F(x) = ((a+\Delta a)x - x^3)\exp(-x^2/b). \tag{2}$$

Here, $x_i(t)$ denotes the time series of the variable in the i-th cubic map, D_a represents the noise strength (mean and standard deviation of $\xi(t)$ are zero and 1.0, respectively; that is, $\xi(t)$ is produced by a normalized Gaussian process), and Δa follows $D_c\zeta$, where D_c and ζ are respectively the error strength and random values following a normalized Gaussian distribution. Owing to the increase in a, the attractor-merging bifurcation arises. Subsequently, a chaos–chaos intermittency appears [31]. The positive value of $c_i(t)$ above a certain strength causes the transition of $x_i(t)$ to the positive attractor region $x_i(t) > 0$. In this study, b was set to 10.0 [31], and the size of the assembly was $N = 512$. The attractor-merging bifurcation is induced by adjusting the internal system parameter a in the chaotic resonance approach. When it is controlled by the additive stochastic noise as in the stochastic resonance approach, a is fixed.

In the memory-storage process for the assembly of cubic maps, the memory signals $c_i(t)$ are input in each cubic map. Before the memory-storage phase, $0 < t < t_s$: t_s and t_e represent the start and end times of the memory storage, respectively, and $c_i(t)$ is set to 0. Initially, $x_i(0)$ is set to a negative value. During memory storage ($t_s \leq t \leq t_e$), the memory signals become $c_i(t) = A\eta_i$ ($A > 0$), where η_i represents a binary memory pattern of "0" or "1" generated using the Poisson process. In the Poisson process, the occurrence probability of "1" corresponds to Λ. After the memory-storage process ($t > t_e$), $c_i(t)$ becomes 0. An example of $c_i(t)$ is shown in Fig.1. The memory-storage patterns $\{X_1, X_2, \cdots, X_i \cdots, X_N\}$ are produced through binarization (i.e., $X_i = 1$ in $x_i(t_e) > 0$ and $X_i = 0$ in $x_i(t_e) \leq 0$). As the parameter set for this study, we used a start time of $t_s = 100$ and end time of $t_e = 200$ in the memory storage as well as $\Lambda = 0.1$ for the Poisson process.

B. EVALUATION INDICES

To evaluate the dynamical system behaviors, we utilized the bifurcation diagram of x_1. In this study, we assumed that the elements of the cubic map assembly exhibit similar temporal behaviors; therefore, we utilized the 1-st element as a typical example. Moreover, to detect the attractor-merging bifurcation and determine whether the attractor is separated or merged in the absence of external noise ($D_a = 0$) and memory signals ($A = 0$), we used the values of $F(f_{\max,\min}) - x_d$. Here, x_d exhibits the separation point for the attractors in the cubic map $x_d = 0$. $f_{\max,\min}$ corresponds to the local maximum and minimum values around $x = x_d$ for the map function, respectively. $F(f_{\max,\min}) - x_d = 0$ corresponds to the attractor-merging bifurcation [31]. Under the condition for $F(f_{\max}) - x_d < 0, F(f_{\min}) - x_d > 0$, in the merged attractor, the orbit hops between the $x_i > x_d$ and $x_i < x_d$ regions.

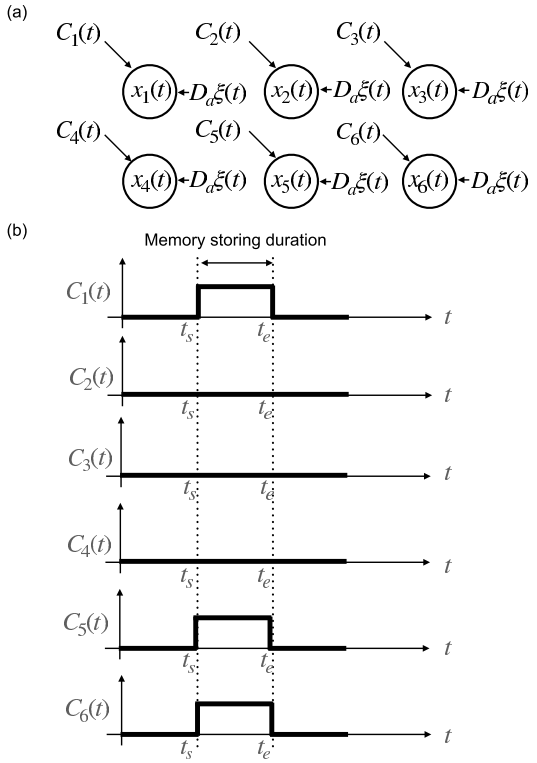

FIGURE 1. Conceptual figures for the memory-storage process in the assembly of cubic maps. (a) Overview of cubic maps $x_i(t)$ applied to memory signals $c_i(t)$ and additive stochastic noise $D_a\xi(t)$. (b) Time series of the memory signal $c_i(t)$ corresponding to the storage pattern. In this example, the assembly size is set to $N = 6$. t_s and t_e correspond to the start and end times for memory storage, respectively.

This indicates that chaos–chaos intermittency appears. The condition for $F(f_{\max}) - x_d > 0$, $F(f_{\min}) - x_d < 0$, and x_i is constrained to either the $x_i > x_d$ or $x_i < x_d$ regions, depending on the initial value of $x_i(0)$.

To determine the chaotic state of x_i, the Lyapunov exponent was calculated as follows [34]:

$$\lambda = \frac{1}{\tau M}\sum_{k=1}^{M}\ln\left(\frac{d^k(t_l=\tau)}{d^k(t_l=0)}\right). \tag{3}$$

Here, $d^k(t_l = 0) = d_0$ $(k = 1, 2, \cdots, M)$ denotes M perturbed initial conditions to $x_i(t)$ applied at $n = n_0 + (k-1)\tau$. The time evolution for $t_l \in [0 : \tau]$ is $d^k(t_l = \tau) = (x_i(t) - x_i'(t))|_{t=t_0+k\tau}$, where $x'(t)$ is a perturbation applied to the orbit. Further, $\lambda > 0$ and $\lambda < 0$ correspond to the chaotic and periodic states, respectively. In this study, the value of λ among N cubic maps is averaged.

To quantify the capability for memory storage, the bit error rate (BER) between the memory pattern η_i and the stored pattern in the assembly of cubic maps X_i $(i = 1, 2, \ldots, N)$ was utilized.

III. RESULTS

A. DEPENDENCY OF SYSTEM BEHAVIOR ON INTERNAL PARAMETER OF CUBIC MAP

First, we demonstrate the dependency of the system behavior on the internal parameter of cubic map a. A bifurcation diagram using positive and negative initial values of $x_1(0)$, Lyapunov exponent λ, and the attractor-merging conditions $F(f_{\max,\min}) - x_d$ is presented in Fig. 2. In $a \lesssim 2.84$, the condition for attractor-separation $(F(f_{\max}) - x_d > 0, F(f_{\min}) - x_d < 0)$ is satisfied. Consequently, the chaotic attractor $(\lambda > 0)$ separates either the positive or negative $x(n)$ region depending on the sign of the initial value $x(0)$. While this separated attractor merges in $a \gtrsim 2.84$ through the attractor-merging bifurcation $(F(f_{\max,\min}) - x_d = 0)$, chaos–chaos intermittency appears $(F(f_{\max}) - x_d < 0, F(f_{\min}) - x_d > 0)$.

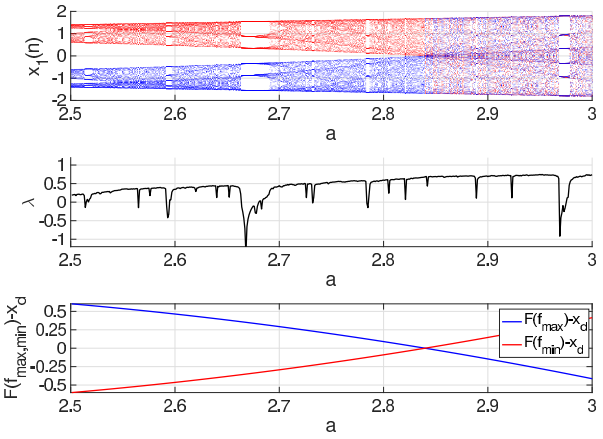

FIGURE 2. System behavior as a function of the internal parameter of the cubic map a. Bifurcation diagram (top panel). The red and blue dots denote the cases with positive and negative initial values of $x_1(0)$, respectively. Lyapunov exponent λ (middle panel). Attractor-merging conditions $F(f_{\max,\min}) - x_d$ (bottom panel). The chaotic attractor ($\lambda > 0$) merges in $a \gtrsim 2.84$, satisfying the attractor-merging condition $(F(f_{\max}) - x_d < 0, F(f_{\min}) - x_d > 0)$.

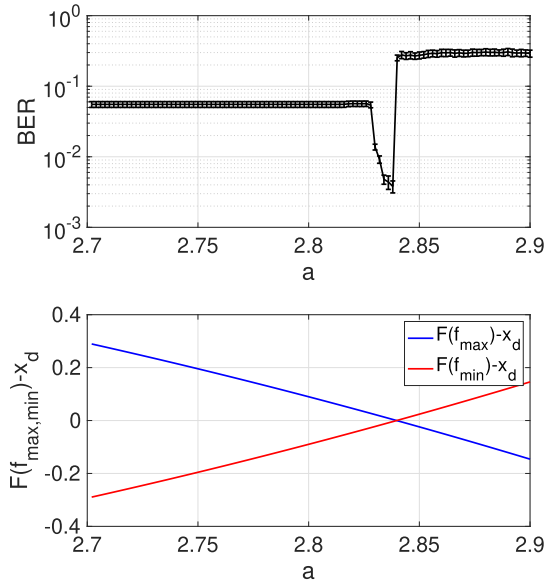

FIGURE 3. Dependency of the capability to store bit-series on the internal parameter a when the input signal strength is $A = 0.01$. The BER between the input bit-series $\{\eta_1, \eta_2, \cdots, \eta_N\}$ and stored bit-series $\{X_1, X_2, \cdots, X_N\}$ (upper panel). The line and bar indicate the mean and standard error among 10 trials with different initial conditions. The attractor-merging conditions $F(f_{\max,\min}) - x_d$ (lower panel). Around the attractor-merging bifurcation $F(f_{\max,\min}) - x_d = 0$ at $a \approx 2.839$, and the BER minimizes to $\approx 4 \times 10^{-3}$. $(D_a = 0, D_c = 0, b = 10)$.

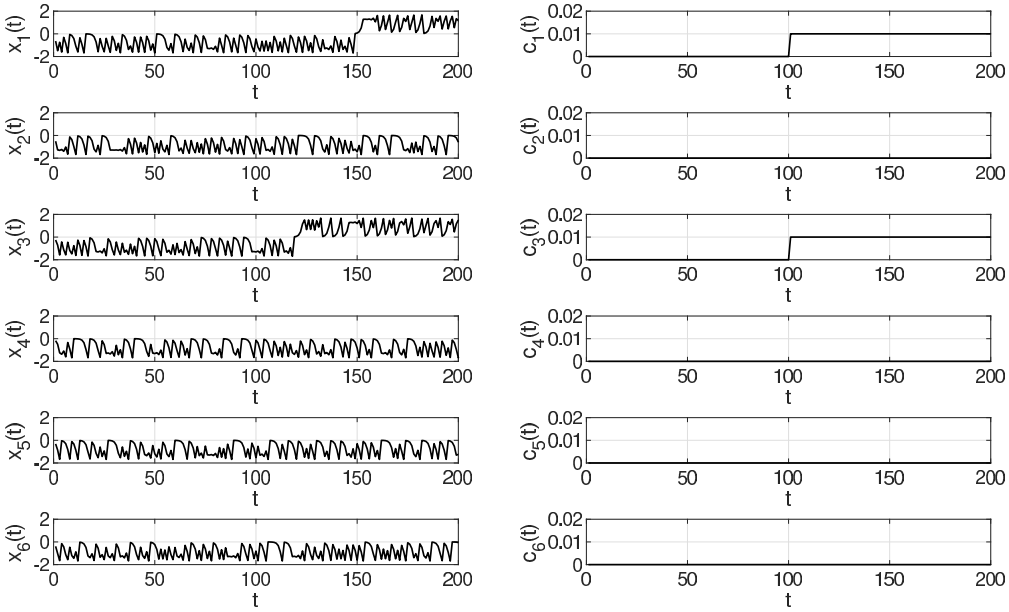

FIGURE 4. Typical example of the transient behaviors of x_i (left parts) and corresponding memory signal c_i (right parts) at the internal parameter $a = 2.839$, where the BER is minimum, as shown in Fig.3. In the 1st and 3rd cubic maps, $x_i(t)$ follows the rising behavior $c_i(t)$ when $t > 100$. The other cubic maps remain in the negative $x_i(t)$ region. In this trial of memory storage patterns, $\eta_{1,3} = 1$, $\eta_{2,4,5,6} = 0$ ($D_a = 0$, $D_c = 0$, $b = 10$, $A = 0.01$).

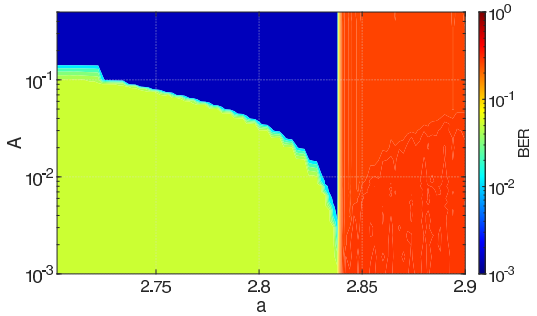

FIGURE 5. Dependency of BER on the input signal strength of A and the internal parameter a. At approximately $a = 2.839$, the attractor-merging bifurcation shown in Fig.2 in $A \gtrsim 4.0 \times 10^{-3}$, BER $\approx 2.0 \times 10^{-3}$ is achieved. ($D_a = 0$, $D_c = 0$, $b = 10$).

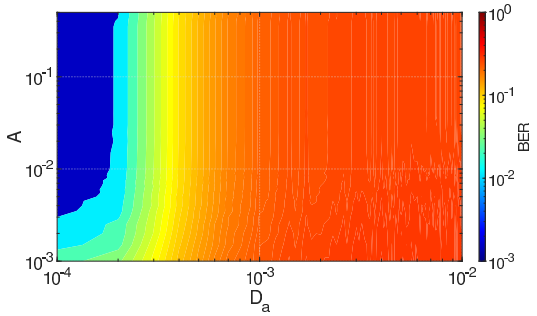

FIGURE 6. Dependency of BER on the input signal strength of A and the strength of the additive stochastic noise of D_a at $a = 2.839$, where BER minimizes under a noise-free condition (shown in Fig. 3). By increasing the noise strength D_a, the lower limit of the input signal strength A, where BER $\approx 2.0 \times 10^{-3}$ is achieved, increases ($b = 10$, $\Delta a = 0$).

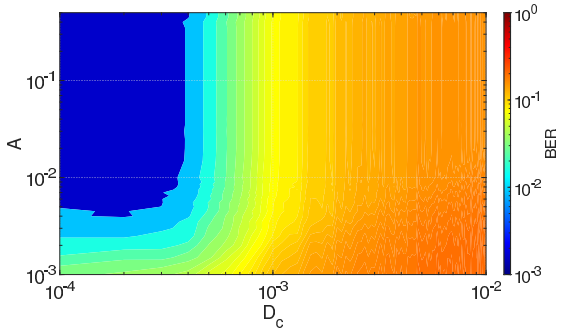

FIGURE 7. Dependency of BER on the input signal strength of A and the strength of the parameter-setting error D_c at $a = 2.839$, where BER minimizes under noise-free ($D_a = 0$) and non-parameter-setting error ($\Delta a = 0$) conditions (shown in Fig. 3). When the strength of the parameter-setting error D_c is increased, the lower limit of the input signal strength A, where BER $\approx 2.0 \times 10^{-3}$ is achieved, increases ($b = 10$, $D_a = 0$).

B. CAPABILITY FOR MEMORY STORAGE BY ADJUSTING INTERNAL CUBIC MAP PARAMETER

1) CAPABILITY UNDER NOISE-FREE AND NO-PARAMETER-SETTING ERROR

We demonstrate the capability of storing the bit-series $\{\eta_1, \eta_2, \cdots, \eta_N\}$ for controlling the attractor-merging bifurcation by adjusting the internal parameter a under a noise-free condition $D_a = 0$ and a non-parameter-setting error $D_c = 0$. In the upper panel of Fig. 3, the BER between the input bit-series $\{\eta_1, \eta_2, \cdots, \eta_N\}$ and stored bit-series $\{X_1, X_2, \cdots, X_N\}$ as a function of the parameter a with an input signal strength of $A = 0.01$ is shown. The lower panel in Fig. 3 shows the attractor-merging conditions $F(f_{\max,\min}) - x_d$ corresponding to the parameter value a in the upper panel of Fig. 3. The result is shown around the attractor-merging bifurcation $F(f_{\max,\min}) - x_d = 0$ at $a \approx 2.839$, and the BER minimizes to $\approx 4 \times 10^{-3}$. This minimization can be construed as a chaotic resonance, where there is a response of the chaos–chaos intermittency against the weak input signal for storing the bit-series. In Fig. 4, a typical example of the time-series of x_i and c_i at the internal parameter $a = 2.839$, where the BER is minimum, is represented

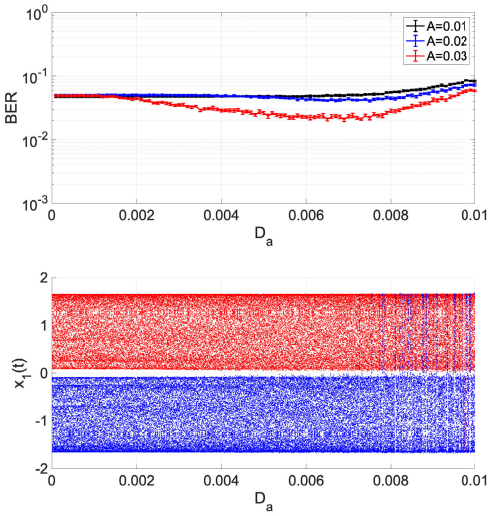

FIGURE 8. Dependency of the capability to store bit-series on the noise strength D_a. BER between the input bit-series and stored bit-series in the cases with signal strengths of $A = 0.01$ (corresponding to the input strength of A, as shown in Fig.3), 0.02, and 0.03 (upper panel). The line and bar indicate the mean and standard error among the 10 trials with different initial conditions. Bifurcation diagram of $x_1(t)$ as a function of the noise strength D under the signal-free condition ($A = 0$) (lower panel). The red and blue dots indicate the cases using positive and negative initial values of $x(0)$, respectively ($a = 2.84$, $b = 10$, $\Delta a = 0$).

(the corresponding BER is shown in the upper panel of Fig.3). In the 1st and 3rd cubic maps, $x_i(t)$ follows the rising behavior $c_i(t) = 0.01$ when $t > 100$. The other cubic maps remain in the negative $x_i(t)$ region set as the initial state of $x_i(0)$ according to $c_i(t) = 0$.

To investigate the sensitivity of adjusting the internal parameter a, the dependence of the BER on the input signal strength of A and the internal parameter a is illustrated in Fig. 5. At approximately $a = 2.839$, the attractor-merging bifurcation, as shown in Fig.2, in $A \gtrsim 4.0 \times 10^{-3}$, BER $\lesssim 2.0 \times 10^{-3}$ is achieved.

2) CAPABILITY UNDER NOISE AND PARAMETER-SETTING ERROR

We investigated the robustness against the additive stochastic noise for high memory storage capability around the attractor-merging bifurcation. Figure 6 shows the dependency of BER on the input signal strength of A and the strength of the additive stochastic noise of D_a at $a = 2.839$, where BER minimizes under a noise-free condition (corresponding to Fig. 3). Increasing the noise strength D_a, the lower limit of the input signal strength A where BER $\approx 2.0 \times 10^{-3}$ is achieved increases. Subsequently, the $A - D_a$ region with BER $\approx 2.0 \times 10^{-3}$ disappears in $D_a \gtrsim 2.0 \times 10^{-4}$.

In addition to the influence of additive stochastic noise, the robustness against the parameter setting error for a was evaluated. Figure 7 shows the dependency of BER on the input signal strength of A and the strength of the parameter-setting error D_c at $a = 2.839$, where BER minimizes under the noise-free ($D_a = 0$) and non-parameter-setting error ($\Delta a = 0$) condition (shown in Fig. 3). When the strength of the parameter-setting error D_c is increased, the lower limit of the input signal strength A, where BER $\approx 2.0 \times 10^{-3}$ is achieved, increases. Eventually,

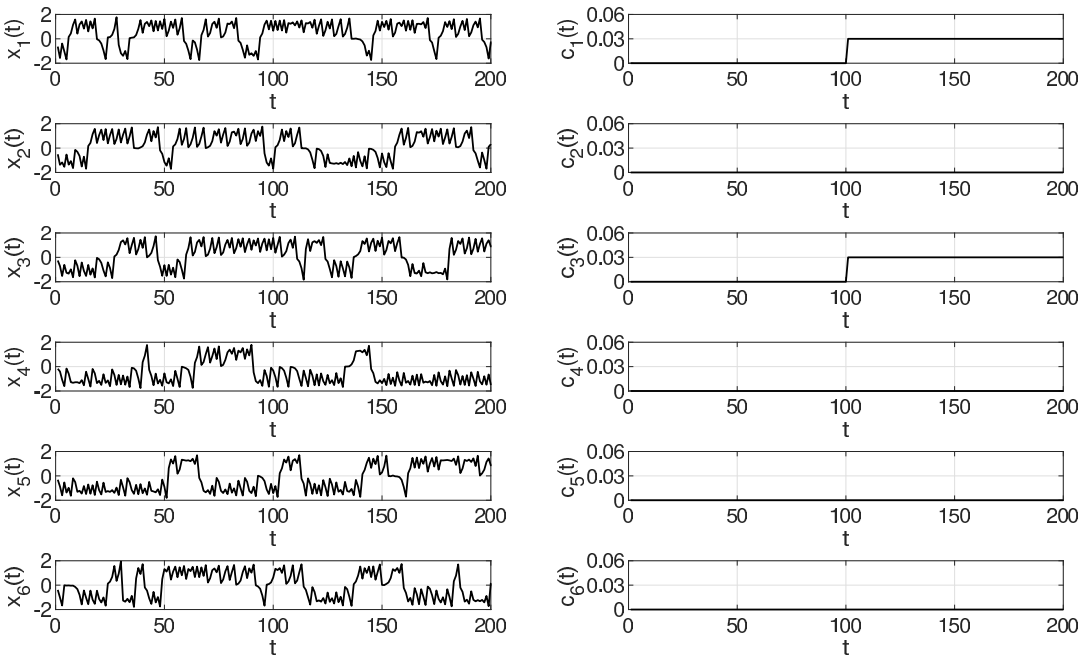

FIGURE 9. Typical example of the transient behaviors of x_i (left parts) and c_i (right parts) for the internal parameter $D_a = 7.0 \times 10^{-3}$, where the BER minimizes as shown in Fig. 8. In contrast to the case where the attractor-merging bifurcation is induced by adjusting the internal system parameter a as shown in Fig.4, the noise-induced chaos–chaos intermittency of $x_i(t)$ does not dominantly follow the rising behavior and remains for $c_i(t)$ when $t > 100$. In this trial for memory-storage patterns, $\eta_{1,3} = 1$, $\eta_{2,4,5,6} = 0$ ($D = 2.8$, $b = 10$, $A = 0.03$, $\Delta a = 0$).

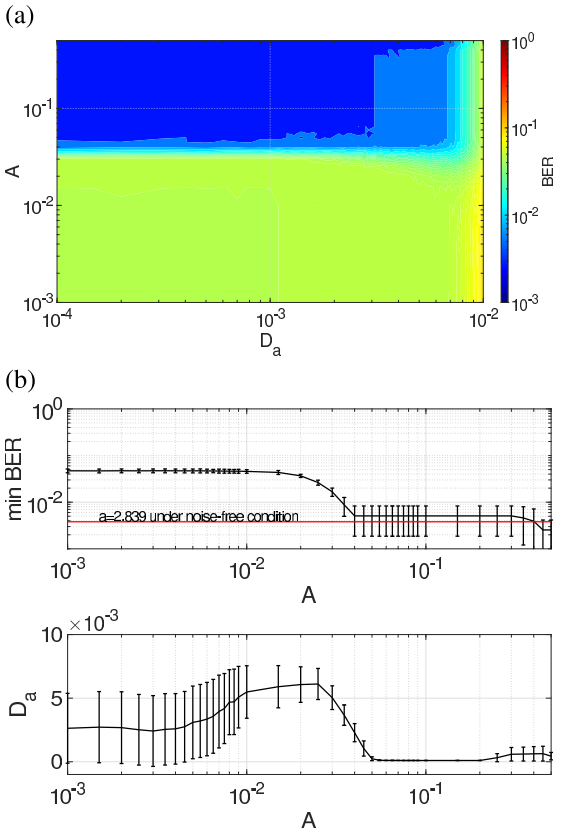

FIGURE 10. (a) Dependency of the BER on the input signal strength of A and the strength of the additive stochastic noise D_a. At approximately $D_a = 7.0 \times 10^{-3}$ where the attractor-merging bifurcation shown in Fig. 8 is $A \gtrsim 0.03$, BER $\approx 2.0 \times 10^{-2}$ is achieved. (b) Input signal strength of A dependency of the minimum BER between $10^{-4} \leq D_a \leq 10^{-2}$ (black line) and BER in $a = 2.839$ under the noise-free condition with $A = 10^{-3}$ (red line) (upper part). A dependency of the appropriate strength of the additive stochastic noise D_a (lower part) ($a = 2.8$, $b = 10$, $\Delta a = 0$).

the $A - D_c$ region with BER $\approx 2.0 \times 10^{-3}$ disappears in $D_c \gtrsim 3.0 \times 10^{-4}$.

C. CAPABILITY TO STORE BIT-SERIES BY ADDITIVE STOCHASTIC NOISE

After evaluating the control of the attractor-merging bifurcation by adjusting the internal parameter a, we investigated the memory storage capability when the attractor-merging bifurcation was induced by an additive stochastic noise ($D_a > 0$). This is similar to the case of the conventional approach using the stochastic resonance mechanism [14], [15]. Considering the evaluation of the dependency of the capability to store bit-series on the noise strength D_a, the upper part of Fig. 8 shows the BER between the input bit-series $\{\eta_1, \eta_2, \cdots, \eta_N\}$ and the stored bit-series $\{X_1, X_2, \cdots, X_N\}$ with a signal strength of $A = 0.01$ (corresponding to the input strength A, as shown in Fig.3). 0.02 and 0.03 are the functions of the noise strength D_a. The lower part of Fig. 8 demonstrates the bifurcation diagram of x_1 as a function of the noise strength D_a under a signal-free condition ($A = 0$). In this evaluation, the parameter-setting error was absent ($\Delta a = 0$). For $A = 0.01$ and 0.02, the BERs monotonously degenerate a noise of increasing strength. When $A = 0.03$, the BER minimizes at $D_a \approx 7.0 \times 10^{-3}$ around the noise-induced attractor-merging bifurcation. Nevertheless, this BER becomes higher (BER$\approx$ 0.02) in comparison with the case where the attractor-merging bifurcation is adjusted by the internal parameter a, as shown in Fig.3 (BER$\approx 4.0 \times 10^{-3}$). Figure 9 shows a typical example of the time-series of x_i and c_i at the noise strength of $D_a = 7.0 \times 10^{-3}$, where the BER is minimum, as shown in Fig.8 ($A = 0.03$). In contrast to the case where the attractor-merging bifurcation is induced by adjusting the internal system parameter a, as shown in Fig.4, the noise-induced chaos–chaos intermittency of $x_i(t)$ does not dominantly follow the rising behavior $c_i(t) = 0.03$ ($i = 1, 3$) and remains at $c_i(t) = 0$ ($i = 2, 4, 5, 6$) when $t > 100$.

To further study the sensitivity of this memory storage to additive stochastic noise, the dependence of the BER on the input signal strength of A and the strength of the additive stochastic noise D_a is illustrated in Fig.10(a). At approximately $D_a = 7.0 \times 10^{-3}$, where the attractor-merging bifurcation occurs (as shown in Fig.8), in $A \gtrsim 0.03$, BER $\lesssim 2.0 \times 10^{-2}$ is achieved. According to the values of BER shown in Fig.10(a), the minimum BER between $10^{-4} \leq D_a \leq 10^{-2}$ at each input signal strength of A are represented in Fig.10(b). In comparison with the case where an adjustment is made to the internal parameter a under a noise-free condition where BER $\approx 4.0 \times 10^{-3}$ in $A = 10^{-3}$, to achieve the same amount of BER, a higher A is needed ($A \gtrsim 0.4$).

IV. DISCUSSION AND CONCLUSION

This study proposed a memory storage mechanism using the high sensitivity of the signal response around the attractor-merging bifurcation in the assembly of cubic maps with chaos–chaos intermittency and evaluated its capability. To control the attractor-merging bifurcation, two approaches were utilized: one was for adjusting the internal cubic map parameter and the other, for applying stochastic noise similar to the conventional approach using the mechanism of stochastic resonance. After comparing the capabilities of both approaches, we confirmed that the former exhibits a high memory storage capability even under weak memory storage input signals. Moreover, this high memory storage ability was maintained under certain levels of existence of stochastic noise and parameter-setting error.

First, we examined the reason why the memory storage capability exhibits a peak around the attractor-merging bifurcation. Under the condition of the attractor-merging bifurcation, the state transition frequency in the autonomous chaos–chaos intermittency is extremely low [31]. The application of an external input signal to the system having low autonomous chaos–chaos intermittencies plays a role in the perturbation for inducing exogenous chaos–chaos intermittencies even under a weak applied signal. Consequently, the state transition that corresponds to memory storage is achieved through the synchronization of chaos–chaos intermittency. This tendency of high synchronization of the

chaos–chaos intermittency is congruent with previous findings in other systems with attractor-merging bifurcation [12], [22], [23]. Therefore, dynamical systems with locally cubic map structures can be utilized to achieve the memory storage systems (reviewed in [12], [26]).

Second, we discussed the memory storage capability when the attractor-merging bifurcation is induced by adjusting the internal parameter a (see Fig. 3) and examined why it is higher than that of the case where the attractor-merging bifurcation is controlled by stochastic noise (see Fig. 8). The additive stochastic noise induces attractor-merging [12]. Through the abovementioned perturbation, the chaos–chaos intermittency, which is unrelated to the input signal for memory storage, also emerges owing to additive noise. Subsequently, the input signal strength A must be set sufficiently higher than the noise strength of D_a. Therefore, the memory storage capability in the case with noise is inferior to the case with internal system parameters. This tendency was also reported in studies that compared the chaotic and stochastic resonances [23], [27]. Utilizing this high memory storage capability in the case with control through the internal parameter a might enable the realization of memory devices with low power consumption.

Third, in contrast, because the approach utilizes stochastic noise, which is similar to stochastic resonance, background noise can be employed. Consequently, the use of background noise leads to low power consumption [14], [15]. However, recent studies on logical circuits used for memory devices driven by the effects of stochastic resonance have indicated that the range of the noise strength required to induce stochastic resonance is narrow [35]. Consequently, because the noise strength required for the induction of stochastic resonance is weak, an approach that applies compensated nonstochastic perturbation was proposed to achieve an adequate level of perturbation for stochastic resonance [35], [36]. The generation of an external perturbation increases power consumption. Therefore, when the noise strength is weak, an alternative solution, which uses an approach for the chaotic resonance controlled by an internal system parameter, should be utilized to overcome the issue related to stochastic resonance, rather than additionally applying the perturbation; as a result, this alternative solution achieves low power consumption.

The limitations of this study are discussed as follows. We investigated the capability of memory storage with chaotic resonance. However, to reveal the relationship between power consumption and storage capability in actual application environments, the electronic circuit of this mechanism should be implemented. Our previous study demonstrated the electronic circuit implementations for chaotic resonances in Chua's circuit [37]; the electronic circuit systems used in the conventional approach that utilizes stochastic resonance [14], [15] might be utilized for the approach for chaotic resonance under the parameter set for chaos–chaos intermittency. The outcome obtained in the aforementioned study can be used in the application of the electronic circuit for storing memory with chaos–chaos intermittency. In the actual circuit implementations using an approach that controls the attractor-merging bifurcation by adjusting the internal system parameter, the memory storage capability is influenced by the stochastic noise and memory-setting error (see Figs. 6 and 7). This influence has also been noted in various types of chaotic systems where chaotic resonance appears [24]. Therefore, the enhancement of its robustness is important for circuit implementation. Moreover, the chaos–chaos intermittency induced by attractor-merging bifurcation is widely observed in various systems, especially neural systems [22]–[24], [32]. Therefore, this approach for chaotic resonance might be applied to neuromorphic computing. Additionally, we proposed the ''reduced region of orbit'' (RRO) feedback method as an alternative approach for the emergence of attractor-merging bifurcation. The chaotic resonance induced by this method has demonstrated high sensitivity against a weak external input signal [22], [23], [31], [38], [39]. Therefore, the capability of the RRO feedback signal must be investigated for memory storage. In future studies, to realize a memory device based on chaotic resonance with low power consumption, the aforementioned aspects must be evaluated.

In summary, this study demonstrated that the chaotic resonance induced by adjusting internal system parameters for the emergence of attractor-merging can detect memory storage signals, even the strength is weak, until the noise- and parameter-setting errors reach a certain level. Moreover, this detection capability is superior to that in the case of the approach induced by additive stochastic noise, which aids the realization of memory devices with extremely low power consumption. Although several limitations remain, our proposed method, which utilizes chaotic resonance, could facilitate the development of memory devices hitherto restricted to the application of stochastic resonance.

REFERENCES

[1] C. S. Hwang, ''Prospective of semiconductor memory devices: From memory system to materials,'' *Adv. Electron. Mater.*, vol. 1, no. 6, Jun. 2015, Art. no. 1400056.

[2] Y. Frégnac, ''Big data and the industrialization of neuroscience: A safe roadmap for understanding the brain?'' *Science*, vol. 358, no. 6362, pp. 470–477, Oct. 2017.

[3] X.-B. Li, N.-K. Chen, X.-P. Wang, and H.-B. Sun, ''Phase-change superlattice materials toward low power consumption and high density data storage: Microscopic picture, working principles, and optimization,'' *Adv. Funct. Mater.*, vol. 28, no. 44, Oct. 2018, Art. no. 1803380.

[4] W. Zhang, R. Mazzarello, M. Wuttig, and E. Ma, ''Designing crystallization in phase-change materials for universal memory and neuro-inspired computing,'' *Nature Rev. Mater.*, vol. 4, no. 3, pp. 150–168, 2019.

[5] A. Lotnyk, M. Behrens, and B. Rauschenbach, ''Phase change thin films for non-volatile memory applications,'' *Nanosc. Adv.*, vol. 1, no. 10, pp. 3836–3857, 2019.

[6] J. Zhu, T. Zhang, Y. Yang, and R. Huang, ''A comprehensive review on emerging artificial neuromorphic devices,'' *Appl. Phys. Rev.*, vol. 7, no. 1, Mar. 2020, Art. no. 011312.

[7] S. K. Garg, C. S. Yeo, and R. Buyya, ''Green cloud framework for improving carbon efficiency of clouds,'' in *Proc. Eur. Conf. Parallel Process.* Berlin, Germany: Springer, 2011, pp. 491–502.

[8] B. Saha, ''Green computing: Current research trends,'' *Int. J. Comput. Sci. Eng.*, vol. 6, no. 3, pp. 467–469, 2018.

[9] C. Jin, X. Bai, C. Yang, W. Mao, and X. Xu, "A review of power consumption models of servers in data centers," *Appl. Energy*, vol. 265, May 2020, Art. no. 114806.
[10] R. Benzi, A. Sutera, and A. Vulpiani, "The mechanism of stochastic resonance," *J. Phys. A, Math. Gen.*, vol. 14, no. 11, p. L453, 1981.
[11] A. Pikovsky, M. Rosenblum, and J. Kurths, *Synchronization: A Universal Concept in Nonlinear Sciences*. Cambridge, U.K.: Cambridge Univ. Press, 2003, vol. 12.
[12] V. S. Anishchenko, V. Astakhov, A. Neiman, T. Vadivasova, and L. Schimansky-Geier, *Nonlinear Dynamics of Chaotic and Stochastic Systems: Tutorial and Modern Developments*. Berlin, Germany: Springer, 2007.
[13] S. Rajasekar and M. A. F. Sanjuán, *Nonlinear Resonances*. Cham, Switzerland: Springer, 2016.
[14] S. A. Ibáñez, P. I. Fierens, R. P. J. Perazzo, G. A. Patterson, and D. F. Grosz, "On the dynamics of a single-bit stochastic-resonance memory device," *Eur. Phys. J. B*, vol. 76, no. 1, pp. 49–55, Jul. 2010.
[15] A. Stotland and M. Di Ventra, "Stochastic memory: Memory enhancement due to noise," *Phys. Rev. E, Stat. Phys. Plasmas Fluids Relat. Interdiscip. Top.*, vol. 85, no. 1, Jan. 2012, Art. no. 011116.
[16] V. Kohar and S. Sinha, "Noise-assisted morphing of memory and logic function," *Phys. Lett. A*, vol. 376, no. 8, pp. 957–962, Feb. 2012.
[17] T. L. Carroll and L. M. Pecora, "Stochastic resonance and crises," *Phys. Rev. Lett.*, vol. 70, no. 5, p. 576, 1993.
[18] T. Carroll and L. Pecora, "Stochastic resonance as a crisis in a period-doubled circuit," *Phys. Rev. E, Stat. Phys. Plasmas Fluids Relat. Interdiscip. Top.*, vol. 47, no. 6, p. 3941, 1993.
[19] S. Sinha and B. K. Chakrabarti, "Deterministic stochastic resonance in a piecewise linear chaotic map," *Phys. Rev. E, Stat. Phys. Plasmas Fluids Relat. Interdiscip. Top.*, vol. 58, no. 6, p. 8009, 1998.
[20] S. Sinha, "Noise-free stochastic resonance in simple chaotic systems," *Phys. A, Stat. Mech. Appl.*, vol. 270, nos. 1–2, pp. 204–214, Aug. 1999.
[21] S. Zambrano, J. M. Casado, and M. A. F. Sanjuán, "Chaos-induced resonant effects and its control," *Phys. Lett. A*, vol. 366, nos. 4–5, pp. 428–432, Jul. 2007.
[22] S. Nobukawa and N. Shibata, "Controlling chaotic resonance using external feedback signals in neural systems," *Sci. Rep.*, vol. 9, no. 1, p. 4990, Dec. 2019.
[23] S. Nobukawa, N. Shibata, H. Nishimura, H. Doho, N. Wagatsuma, and T. Yamanishi, "Resonance phenomena controlled by external feedback signals and additive noise in neural systems," *Sci. Rep.*, vol. 9, no. 1, pp. 1–15, Dec. 2019.
[24] H. Doho, S. Nobukawa, H. Nishimura, N. Wagatsuma, and T. Takahashi, "Transition of neural activity from the chaotic bipolar-disorder state to the periodic healthy state using external feedback signals," *Frontiers Comput. Neurosci.*, vol. 14, p. 76, Aug. 2020.
[25] Y. He, Y. Fu, Z. Qiao, and Y. Kang, "Chaotic resonance in a fractional-order oscillator system with application to mechanical fault diagnosis," *Chaos, Solitons Fractals*, vol. 142, Jan. 2021, Art. no. 110536.
[26] S. Nobukawa and H. Nishimura, "Synchronization of chaos in neural systems," *Frontiers Appl. Math. Statist.*, vol. 6, p. 19, Jun. 2020.
[27] H. Nishimura, N. Katada, and K. Aihara, "Coherent response in a chaotic neural network," *Neural Process. Lett.*, vol. 12, no. 1, pp. 49–58, 2000.
[28] V. S. Anishchenko, M. A. Safonova, and L. O. Chua, "Stochastic resonance in the nonautonomous Chua's circuit," *J. Circuits, Syst. Comput.*, vol. 3, no. 2, pp. 553–578, Jun. 1993.
[29] S. Nobukawa, H. Nishimura, and N. Katada, "Chaotic resonance by chaotic attractors merging in discrete cubic map and chaotic neural network," *IEICE Trans. A*, vol. 95, no. 4, pp. 357–366, 2012.
[30] S. Nobukawa, H. Nishimura, and T. Yamanishi, "Evaluation of chaotic resonance by Lyapunov exponent in attractor-merging type systems," in *Proc. Int. Conf. Neural Inf. Process.* Cham, Switzerland: Springer, 2016, pp. 430–437.
[31] S. Nobukawa, H. Nishimura, T. Yamanishi, and H. Doho, "Controlling chaotic resonance in systems with chaos-chaos intermittency using external feedback," *IEICE Trans. Fundam. Electron., Commun. Comput. Sci.*, vol. 101, no. 11, pp. 1900–1906, 2018.
[32] N. Shibata and S. Nobukawa, "Synchronization of chaos–chaos intermittency controlled by external feedback and stochastic noise," in *Proc. ISCIE Int. Symp. Stochastic Syst. Theory Appl.*, 2020, pp. 17–22.
[33] S. Nobukawa, N. Wagatsuma, H. Nishimura, K. Inagaki, and T. Yamanishi, "Novel approach for memory storage systems with chaos-chaos intermittency," in *Proc. Int. Conf. Emerg. Techn. Comput. Intell. (ICETCI)*, Aug. 2021, pp. 123–128.
[34] T. S. Parker and L. Chua, *Practical Numerical Algorithms for Chaotic Systems*. New York, NY, USA: Springer, 2012.
[35] B. Yang, X. Zhang, and M.-K. Luo, "When noise-free logical stochastic resonance occurs in a bistable system," *Nonlinear Dyn.*, vol. 87, no. 3, pp. 1957–1965, Feb. 2017.
[36] A. Gupta, A. Sohane, V. Kohar, K. Murali, and S. Sinha, "Noise-free logical stochastic resonance," *Phys. Rev. E, Stat. Phys. Plasmas Fluids Relat. Interdiscip. Top.*, vol. 84, Nov. 2011, Art. no. 055201.
[37] S. Nobukawa, H. Doho, N. Shibata, H. Nishimura, and T. Yamanishi, "Chaos–chaos intermittency synchronization controlled by external feedback signals in Chua's circuits," *IEICE Trans. Fundam. Electron., Commun. Comput. Sci.*, vol. 103, no. 1, pp. 303–312, 2020.
[38] S. Nobukawa, H. Nishimura, T. Yamanishi, and H. Doho, "Induced synchronization of chaos–chaos intermittency maintaining asynchronous state of chaotic orbits by external feedback signals," *IEICE Trans. Fundam. Electron., Commun. Comput. Sci.*, vol. 102, no. 3, pp. 524–531, 2019.
[39] S. Nobukawa, N. Wagatsuma, and H. Nishimura, "Chaos–chaos intermittency synchronization induced by feedback signals and stochastic noise in coupled chaotic systems," *IEICE Trans. Fundam. Electron., Commun. Comput. Sci.*, vol. 103, no. 9, pp. 1086–1094, 2020.

SOU NOBUKAWA (Member, IEEE) graduated from the Department of Physics and Earth Sciences, University of Ryukyus, in 2006. He received the Ph.D. degree from the University of Hyogo, in 2013. He is currently an Associate Professor with the Department of Computer Science, Chiba Institute of Technology. His research interests include chaos/bifurcation and neural networks. He is a member of INNS, IEICE, JNNS, IPSJ, SICE, and ISCIE. He was awarded the SICE encouraging prize in 2016; the Young Researcher Award by the IEEE Computational Intelligence Society Japan Chapter; the Best Paper Award of the 29th Symposium on Fuzzy, Artificial Intelligence, Neural Networks and Computational Intelligence in 2019; and the Excellent Research Award by the Japanese Neural Network Society/the Best Paper Award of SSI in 2021.

NOBUHIKO WAGATSUMA received the B.S., M.S., and Ph.D. degrees from the University of Tsukuba, in 2004, 2006, and 2009, respectively. He is currently a Lecturer with the Faculty of Science, Department of Information Science, Toho University. His research interests include visual attention and computational neuroscience. He was awarded the Best Paper Award in 2020 and the Excellent Research Award in 2021 by the Japanese Neural Network Society.

HARUHIKO NISHIMURA (Member, IEEE) graduated from the Department of Physics, Shizuoka University, in 1980. He received the Ph.D. degree from Kobe University, in 1985. He is currently a Professor Emeritus and a Specially Appointed Professor with the Graduate School of Applied Informatics, University of Hyogo. His research interests include intelligent systems science based on several architectures such as neural networks and complex systems. He is also engaged in research in biomedical, healthcare, and high-confidence sciences. He is a member of IEICE, IPSJ, ISCIE, JNNS, and other organizations. He was awarded the ISCIE Paper Prize in 2001 and the JSKE Paper Prize in 2010.

KEIICHIRO INAGAKI (Member, IEEE) received the Ph.D. degree in engineering from Chubu University, in 2007. From 2007 to 2009, he worked as a Postdoctoral Researcher with the Department of Anatomy and Neurophysiology and the Department of Otolaryngology, Washington University School of Medicine, St. Louis. From 2009 to 2013, he was a Postdoctoral Researcher with RIKEN. In 2013, he joined the Department of Robotic Science and Technology, Chubu University. From 2013 to 2014, he worked as an Assistant Professor. Since 2014, he has been working as a Senior Assistant Professor.

TERUYA YAMANISHI received the M.S. degree in science education and the Ph.D. degree in physics from Kobe University, in 1991 and 1994, respectively. He is currently a Professor with the Fukui University of Technology, where he studies mathematical information science of the brain and develops tools to optimize the behavior of autonomous robots.